3P-40

Proceedings of Symposium on Ultrasonic Electronics, Vol. 31 (2010) pp. 535-536
6-8 December, 2010

For a practical use of thermoacoustic system – Effect of local change in tube material on energy conversion –

熱音響システムの実用化に向けて
– 局所的な管材質変化がエネルギー変換に与える影響 –

Kazuki Sahashi[1‡], Shin-ichi Sakamoto[2], Yoshiaki Watanabe[3] ([1]Grad. School of Eng., Doshisha Univ.; [2]School of Eng., Univ. of Shiga Pref.; [3]School of Life and Medical Sciences, Doshisha Univ.)
佐橋 一輝[1‡], 坂本 眞一[2], 渡辺 好章[3] ([1]同志社大 工, [2]滋賀県立大 工, [3]同志社大 生命医科)

1. Introduction

Increasingly, earth environment deterioration caused by global warming and fuel source depletion is viewed with anxiety. At present, loop-tube type thermoacoustic cooling systems[1] (loop-tubes) have attracted attention as cooling systems that can convert unused energy such as waste heat and solar heat. The system has two heat–sound energy conversion components: a prime mover and a heat pump. Improvement of energy conversion efficiency at these parts is an obstacle to the practical use of loop-tubes.

Using a Phase Adjuster[2] (PA) improves the loop-tube energy conversion efficiency. Great improvement of ΔI_{PM}, the quantity of sound intensity amplification, can be made at a prime mover regenerator.[3] Moreover, the associated quantity of high sound intensity attenuation, ΔI_{PA}, was formed. The reasons for ΔI_{PM} improvement must be elucidated for design of an optimum PA setting in a loop-tube and for more improved energy conversion efficiency. As reasons for ΔI_{PM} improvement, formation of ΔI_{PA}, reflection of acoustic wave at both ends of PA, and an increase in particle velocity in PA are considered.

This report describes our specific examination of ΔI_{PA} as a ΔI_{PM} improvement factor. The relation between ΔI_{PA} and ΔI_{PM} is discussed using information from increased dissipation of acoustic waves resulting from local change in tube material from stainless steel to acrylic.

2. Acoustic amplification concept

The quantity of sound intensity amplification at the prime mover regenerator, ΔI_{PM}, changes along with system conditions. That value reflects the energy conversion efficiency at the prime mover. The high-temperature and low-temperature heat exchangers set in both ends of the regenerator have temperatures defined respectively as T_H and T_C. When the ratio of T_H to T_C reaches the oscillation temperature ratio, self-excited oscillation begins in the tube. Thereby, the temperature at the upper end of the regenerator and the distribution of phase difference between sound pressure and particle velocity in the prime mover regenerator change; ΔI_{PM} also changes. The acoustic wave amplitude increases and finally stops when $\dot{E}$, the quantity of energy dissipation of the system per unit of time, equals the products of ΔI_{PM} and the cross-sectional area. Atchley shows $\dot{E}$ as equation (1)[4].

$$\dot{E} = \dot{E}_{pipe} + \dot{E}_{reg.} - \dot{E}_{\Delta T}, \qquad (1)$$

where $\dot{E}_{pipe}$ and $\dot{E}_{reg.}$ respectively denote energy dissipation at the duct and regenerator. Energy production by the thermoacoustic effect, $\dot{E}_{\Delta T}$, becomes a finite value when a thermal gradient exists in a regenerator. Local change in the tube material can increase $\dot{E}_{pipe}$.

3. Experimental conditions

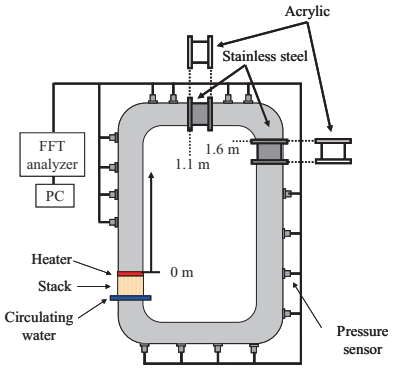

Fig. 1 Schematic of the experimental system.

A schematic of the experimental system is presented in **Fig. 1**. For this experiment, we used a cylindrical loop-tube made of stainless steel, with total length of 3.3 m and inner diameter of 42 mm. The system was filled with air at atmospheric pressure. The 50-mm-long regenerator at the prime mover has honeycomb ceramic cells (900 cell/inch^2). The heat pump was intentionally eliminated because we focused on the prime mover. A spiral-type electric heater inserted at the top of the regenerator served as the heat source; a heat exchanger to maintain the system at room temperature was placed at the lower part of the regenerator. Electric power of 330 W was supplied to the electric heater.

In these conditions, we measured sound pressure in the tube. Then, the tube material was changed from stainless steel to acrylic at the area of 0.1 m, from 1.1 m to 1.2 m, or from 1.6 m to 1.7 m, with their origin at a heater set position. These positions were an optimum PA setting position and a pressure antinode position respectively.

The sound pressure in the tube was measured using the pressure sensors (PCB Inc.). From the measured pressure, the sound intensity distribution in the tube was calculated using a two-sensor power method[5]. Then, the

dtk0158@mail4.doshisha.ac.jp

particle velocity and the phase difference between sound pressure and particle velocity were calculated.

4. Experimental results and considerations

The sound intensity distribution in the tube is presented in **Fig. 2**. ΔI_{AC}, the increased quantity of sound intensity attenuation at acrylic setting position, was verified when setting acrylic in a part of this system. When setting acrylic at 1.1 m and 1.6 m, the respective ΔI_{AC} values were about 30 W/m^2 and 16 W/m^2. Furthermore, $\Delta I_{PM}$was 160 W/m^2 when we used stainless steel as the tube material. When setting acrylic at 1.1 m and 1.6 m, the respective ΔI_{PM} values were about 480 W/m^2 and 175 W/m^2, which were about 3.0 times and 1.1 times the value obtained using stainless steel.

A cause of the ΔI_{PM} difference was considered in terms of acoustic wave amplification. As described in chapter 2, acoustic wave amplification stops when $\dot{E}$ equals the products of ΔI_{PM} and the cross-sectional area of the tube. In this report, ΔI_{AC} formed by local change in tube material from stainless steel to acrylic contributes to increased $\dot{E}$. Therefore, it is expected that ΔI_{PM} with acrylic is greater than ΔI_{PM} with stainless steel because ΔI_{PM} amplification stops when ΔI_{PM} equals $\dot{E}$. Furthermore, acoustic wave amplification with acrylic is expected to stop earlier than with stainless steel because $\dot{E}$ with acrylic is higher than that with stainless steel. Therefore, it is expected that the value of sound intensity at the hot end of a regenerator with acrylic is lower than that with stainless steel, as confirmed from the sound intensity distribution with acrylic at 1.6 m. However, results show that the value of sound intensity at the hot end of the regenerator with acrylic at 1.1 m is higher than that with stainless steel. Therefore, we focused on the phase difference distribution between sound pressure and particle velocity in the tube, as **Fig. 3** shows. The phase difference in the tube changed; the phase difference in the prime mover regenerator is expected to approach 0° with acrylic at 1.1 m. Therefore, it is expected that high acoustic wave amplification with acrylic at 1.1 m is achievable by setting up higher ΔI_{PM} than in other conditions because ΔI_{PM} depends on the phase difference in the prime mover regenerator. Moreover, a cause of change in the phase difference according to the change in the acrylic setting position was considered as below. **Figure 4** shows the acoustic impedance distribution in the tube, which is the value of sound pressure divided by the particle velocity, with stainless steel. Increased energy dissipation by local change in the tube material increases the acoustic impedance at a part of the tube. For the case of 1.1 m, acrylic was set in a position of low acoustic impedance. Therefore, the sound field is expected to be affected, breaking the standing wave, which might cause the phase difference in the prime mover regenerator to approach 0°. However, for the case of 1.6 m, the phase difference distribution in the tube is not expected to change because acrylic was set in a position of high acoustic impedance.

5. Summary

This report described formation of ΔI_{AC} by local change in tube material and explained effects of ΔI_{AC} on ΔI_{PM}. Results show that ΔI_{PM}increased in accordance with ΔI_{AC} formation. Results show that the phase difference varied according to the change in the setting position of the acrylic, and that ΔI_{PM}yielded a large change.

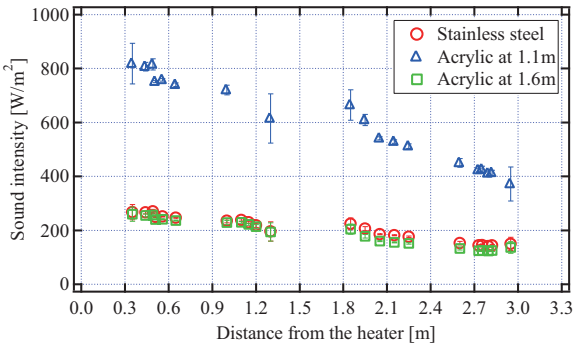

Fig. 2 Sound intensity distribution with stainless steel and acrylic.

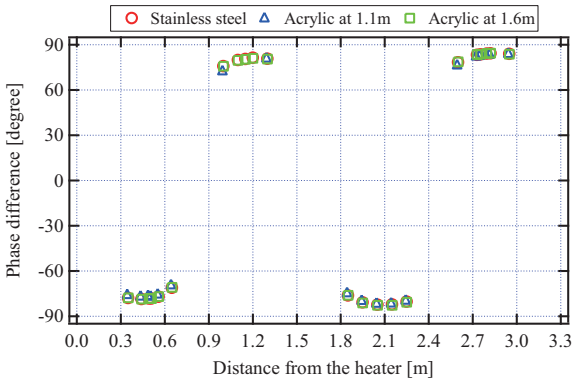

Fig. 3 Phase difference distribution between sound pressure and particle velocity with stainless steel and acrylic.

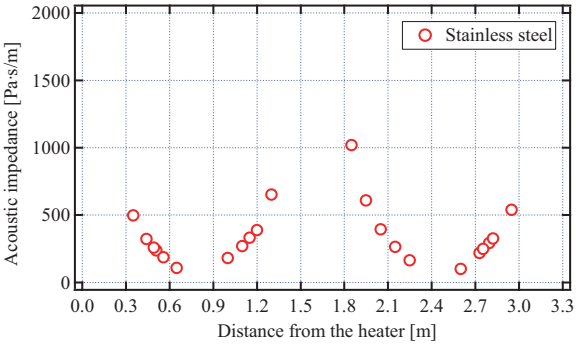

Fig. 4 Acoustic impedance distribution with stainless steel.

Acknowledgment

This work was partially supported by a Grant-in-Aid for Young Scientists (A), (B).

References

1. A. Tominaga: *Fundamental Thermoacoustic* (Uchida Roukakuho Publishing, 1998).
2. S. Sakamoto *et al*: Jpn. J. Appl. Phys. **467B** (2007) 4951-4955.
3. S. Komiya *et al*: IEICE technical report. Ultrasonics. **108** 410 (2009) 75-80.
4. A. Atchley: J. Acoust. Soc. Am. **95** (1994) 1661.
5. T. Biwa *et al*: J. Acoust. Soc. Am. **124** 3 (2008) 1584-1590.